Monolithic Germanium PIN Waveguide Photodetector Operating at 2 μm Wavelengths

Ziqiang Zhao, Chongpei Ho, Qiang Li, Kasidit Toprasertpong, Shinichi Takagi and Mitsuru Takenaka
Department of Electrical Engineering and Information Systems, The University of Tokyo, 7-3-1 Hongo, Bunkyo-ku, Tokyo, 113-8656, Japan
zhaozq@mosfet.t.u-tokyo.ac.jp

Abstract: We demonstrated Ge PIN waveguide photodetector operating at 2 μm wavelengths monolithically integrated on Ge-on-insulator platform. Despite at sub-bandgap wavelength, 500-μm-long photodetector exhibited 0.25 A/W responsivity at -5 V, attributable to the defect-mediated detection mechanism. © 2020 The Author(s)

OCIS codes:(130.3060) Infrared; (130.3120) Integrated optics devices; (130.3130) Integrated optics materials; (250.0040) Detectors.

1. Introduction

The demands for high-speed and large-channel-capacity data transmission have been strongly escalated by the emergence of 5G technologies. With the development of low-loss hollow-core optical fibers and thulium doped fiber amplifier (TDFA) [1], the interests for opening a new optical communication window at 2 μm wavelengths has intensified. To realize optical fiber communication at 2 μm wavelengths, mid-infrared (MIR) Si photonics have been developed recently [2]. In particular, Si-based monolithic photodetectors (PDs) operating at MIR have been demonstrated based on the defect-mediated detection mechanism using Si divacancy or Si:Zn defects [3-6]. However, the inefficient detection in defect-mediated Si PDs needs a long device and/or high voltage for achieving considerable responsivity, impeding practical usages.

In this work, we have proposed to use Ge instead of Si for photodetection at 2 μm wavelengths. Since narrow-gap Ge has much greater intrinsic carrier density than Si, we expect the substantial enhancement in defect-mediated detection efficiency according to SRH theory [7]. To examine the capability of the photodetection at 2 μm wavelengths in Ge, we fabricated a Ge waveguide with a lateral PIN junction on a Ge-on-insulator (GeOI) platform [8] as shown in Fig. 1. We found that the 500-μm-long Ge PIN waveguide exhibited high responsivity of 0.25 A/W with -5 V bias voltage at 1960 nm wavelengths, enabling a new strategy of the photodetection in 2 μm communication band.

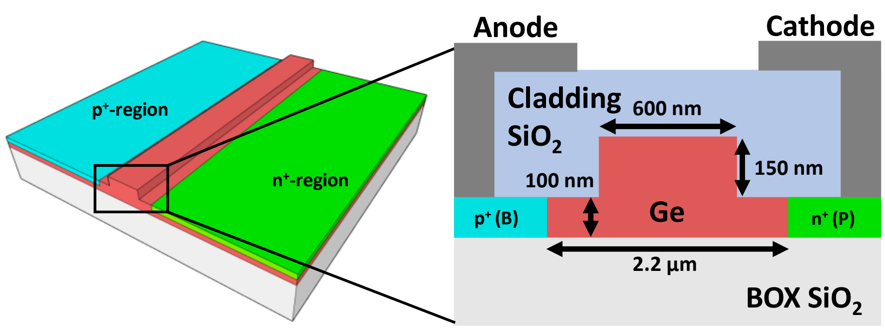

Fig.1. Schematic of Ge PIN waveguide PD on GeOI platform.

2. Design and fabrication

Figure 1 illustrates a schematic of the Ge PIN waveguide PD on a GeOI wafer. We have investigated the GeOI platform for MIR photonics, enabling Ge rib/strip waveguide like as Si photonics [8,9]. We prepared a 600-nm-wide, 250-nm-high Ge rib waveguide with a lateral PIN junction. The gap between the p$^+$- and n$^+$-doped regions was designed to be 2.2 μm to avoid the free-carrier absorption of the doped regions [10].

A fabrication procedure of a Ge waveguide PD is shown in Fig. 2 (a). First, we prepared a GeOI wafer by Smart Cut^{TM}. A 4-inch bulk n-Ge wafer with impurity density of ~10^{15} cm^{-3} was firstly pre-cleaned, followed by 100-nm-thick SiO_2 deposition by plasma-enhanced chemical vapor deposition (PECVD). After that, hydrogen (H^+) ion implantation with dose of 4×10^{16} cm^{-2} at 80 keV was applied on the prepared Ge wafer. A 4-inch Si handling wafer with a 2-μm-thick SiO_2 buried oxide (BOX) layer was also prepared. After removing the SiO_2 layer on the top of the Ge wafer, we deposited 5-nm-thick Al_2O_3 by atomic layer deposition (ALD) on both Ge wafer and Si handling wafer, followed by wafer bonding process. First annealing at 250 °C was performed to strengthen bonding and second annealing at 400 °C was introduced to accelerate the accumulation of hydrogen platelets for wafer splitting. The Ge thickness after splitting was around 650 nm. Ge layer was then planarized and thinned to around 500 nm by chemical mechanical polishing (CMP) followed by 500 °C annealing in high vacuum ambient for 1 h to improve the Ge crystal quality. Finally, the Ge layer was thinned to 250 nm by dry etching. Ge waveguides were formed on a GeOI wafer by electron-beam lithography and dry etching with CF_4. Then, a 10-nm-thick SiO_2 capping layer was deposited by PECVD for boron (B) implantation. Afterward, an additional 100-nm-thick SiO_2 hard mask was carried out for phosphorus (P) doping. We applied a solid-phase doping from P-doped spin-on-glass (SOG) instead of implantation. The activation of B and the diffusion of P were simultaneously carried out at 650 °C for 1 min in N_2 ambient. As a result, a high doping level of approximately 10^{19} cm^{-3} for both n^+- and p^+-regions were obtained. After deposition of a 400-nm-thick SiO_2 cladding layer and via opening, Ni/Al electrodes were formed. Figure 2(b) shows a plan-view of the fabricated Ge waveguide PD with a 500 µm-long PIN junction.

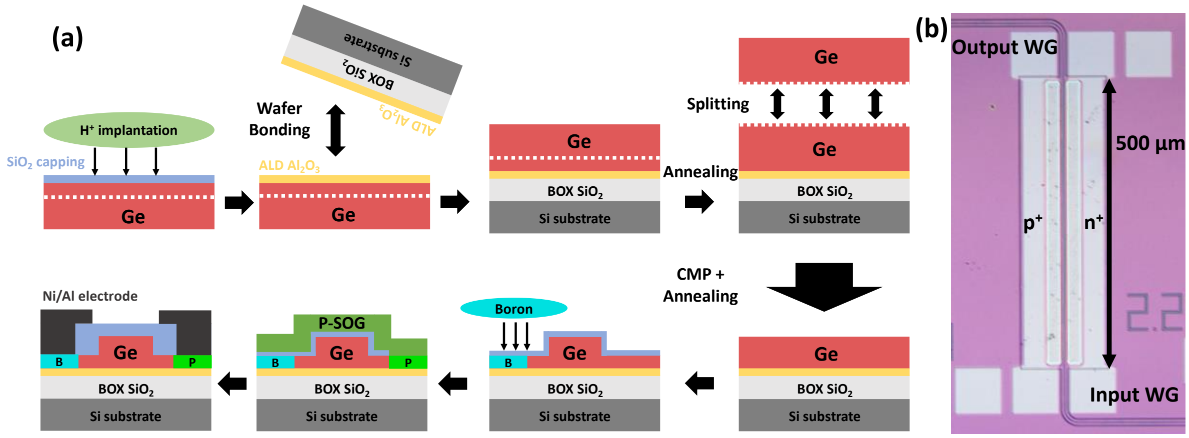

Fig. 2. (a) Process flow and (b) plan-view of Ge PIN waveguide PD.

3. Experimental results

We firstly evaluated the propagation loss of the fabricated Ge passive waveguide. An amplified spontaneous emission (ASE) light source at 2 µm wavelengths based on TDFA was coupled into the waveguides through a grating coupler. The output light was coupled back to a single-mode fiber through a grating coupler for power measurement. As shown in Fig. 3(a), the propagation loss of a 600-nm-wide passive Ge waveguide was 1.6 dB/mm which was dominated by sidewall scattering. We further evaluated the propagation loss of the Ge PIN waveguide. We observed an extra optical loss of 3.8 dB/mm as shown in Fig. 3(b). Since we designed the device to make the free-carrier absorption from the doped regions negligible, the extra optical loss might be attributable to defect generation during the PIN junction formation. In particular, the SOG process induces thermal stress during high-temperature diffusion [11], which might degrade the crystal quality of the Ge layer. Figure 3(c) is the I-V characteristics of a 500-µm-long Ge PIN waveguide PD w/ and w/o illumination of ASE light whose center wavelength was 1960 nm. By taking into account the coupling loss of the grating coupler and the propagation loss of the access Ge passive waveguide, the intrinsic input power into

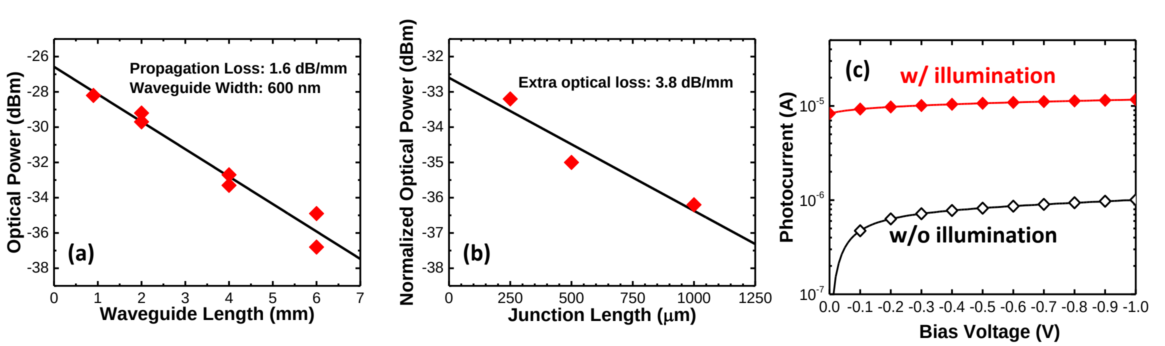

Fig.3. (a) Propagation loss of 600-nm-wide passive Ge waveguide and (b) extra propagation loss in Ge PIN waveguide. (c) I-V characteristic of a 500-µm-long Ge PIN waveguide PD w/ and w/o illumination of ASE light at center wavelength of 1960 nm.

the waveguide PD was approximately -12 dBm. We found substantial photocurrent of approximately 10.7 µA at -1 V bias despite at sub-bandgap wavelength, showing the feasibility of the photodetection at 2 µm wavelengths in the Ge PIN waveguide.

We further evaluated the responsivity with extended range of bias voltage from 0 V to -5 V. As shown in Fig. 4(a), the responsivity for a 500-µm-long Ge PD reached 0.25 A/W when a bias voltage was -5 V. The estimated quantum efficiency was approximately 16%. Figure 4(b) shows benchmark of the responsivity of defect-mediated MIR PDs as a function of device length when a bias voltage was -5 V. As we expected, the presented Ge PIN waveguide PD exhibited rather high responsivity despite relatively short device length.

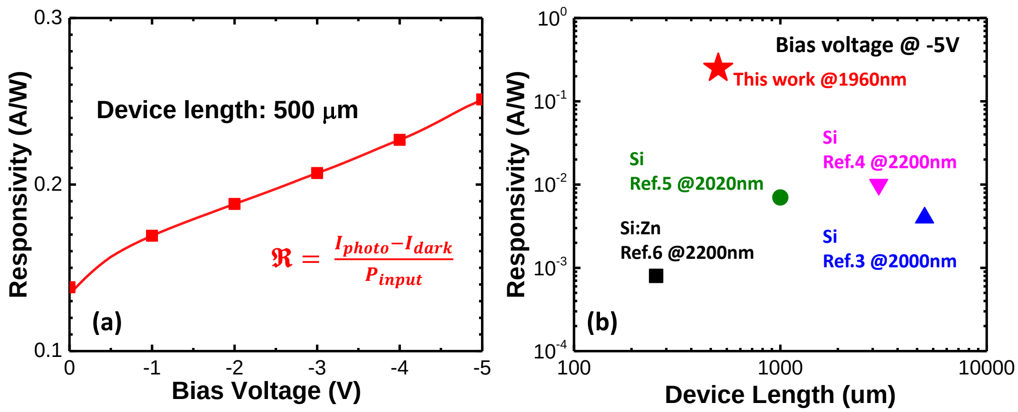

Fig.4. (a) Responsivity of a 500-µm-long Ge PIN waveguide PD with reversed bias voltage from 0 V to -5 V and (b) benchmark responsivity of defect-mediated MIR PDs as a function of device length.

4. Conclusions

We have demonstrated photodetection at 2 µm wavelengths using Ge PIN waveguide formed on a GeOI platform, possibly due to the defect-mediated detection mechanism. The 500-µm-long PD exhibited responsivity of 0.25 A/W at -5 bias, which is rather higher sensitivity than Si defect-mediated PDs. The present result suggests the superiority of a Ge defect-mediated PD at 2 µm and further longer wavelengths.

5. Acknowledgements

This work was partly commissioned by the New Energy and Industrial Technology Development Organization (NEDO).

6. References

[1] G. Fatima and B. Corbett, "Time to Open the 2-µm Window?," Opt. Photonics News **30,** 42-47 (2019).
[2] H. Lin, Z. Luo, T. Gu, L. C. Kimerling, K. Wada, A. Agarwal and J. Hu, "Mid-infrared integrated photonics on silicon: a perspective.," Nanophotonics **7,** 393-420 (2017).
[3] D. J. Thomson, L. Shen, J. J. Ackert, E. Huante-Ceron, A. P. Knights, M. Nedeljkovic, A. C. Peacock and G. Z. Mashanovich, "Optical detection and modulation at 2µm-2.5 µm in silicon.," Opt. Express **20,** 10825-10830 (2014).
[4] B. Souhan, R. R. Grote, C. P. Chen, H. C. Huang, J. B. Driscoll, M. Lu, A. Stein, H. Bakhru, K. Bergman, W. M. J. Green and R. M. Osgood, "Si^+-implanted Si-wire waveguide photodetectors for the mid-infrared.," Opt. Express **22,** 27415-27424 (2014).
[5] J. J. Ackert, D. J. Thomson, L. Shen, A. C. Peacock, P. E. Jessop, G. T. Reed, G. Z. Mashanovich and A. P. Knights, "High-speed detection at two micrometres with monolithic silicon photodiodes.," Nat. Photonics **9,** 393 (2015).
[6] R. R. Grote, B. Souhan, N. Ophir, J. B. Driscoll, K. Bergman, H. Bahkru, W. M. J. Green and R. M. Osgood, "Extrinsic photodiodes for integrated mid-infrared silicon photonics.," Optica **1,** 264-267 (2014).
[7] M. J. Keevers and M. A. Green, "Efficiency improvements of silicon solar cells by the impurity photovoltaic effect.," J. Appl. Phys. **75,** 4022-4031 (1994).
[8] J. Kang, M. Takenaka and S. Takagi, "Novel Ge waveguide platform on Ge-on-insulator wafer for mid-infrared photonic integrated circuits.," Opt. Express **24,** 11855-11864 (2016).
[9] J. Kang, S. Takagi and M. Takenaka, "Design and characterization of Ge passive waveguide components on Ge-on-insulator wafer for mid-infrared photonics.," Jpn. J. Appl. Phys. **57,** 042202 (2018).
[10] Y. Kim, J. Fujikata, S. Takahashi, M. Takenaka and S. Takagi, "Demonstration of record-low injection-current variable optical attenuator based on strained SiGe with optimized lateral pin junction.," Opt. Express **23,** 12354-12361 (2015).
[11] V. Boldrini, S. M. Carturan, G. Maggioni, E. Napolitani, D. R. Napoli, R. Camattari and D. De Salvador, "Optimal process parameters for phosphorus spin-on-doping of germanium.," Appl. Surf. Sci. **392,** 1173-1180 (2017).